A bubble formation in the two-phase system *

Karel Fraňa[1 [0000-0002-2319-7833]], Shehab Attia[1], and Jörg Stiller[2]

Technical University of Liberec, Studentská 2, 461 17 Liberec, Czech Republic,
karel.frana@tul.cz, shehab.attia@tul.cz
Technische Universität Dresden, Institut für Strömungsmechanik 01062, Dresden,
Germany, joerg.stiller@tu-dresden.de

Abstract. The formation of the bubbles in the liquid was examined numerically and results were successfully compared with the results provided by experiments. The study covered two different patterns defined by different Morton numbers or gas flow rates. The unsteady three dimensional calculations were carried out in code OpenFoam with the volume of fluid approach. Numerical results were in a good match to the experiments in respect to bubble shapes, diameters and Reynolds numbers. More accurate comparison was found for lower gas flow rate then for the higher one. The main reason can be that under higher gas flow rate, a complex flow behavior between gas bubbles and surrounding liquid flow is created which worsens the accuracy of calculations. The main important output of the study was a comparison of the bubble diameters in time. Especially for higher gas flow rates, bubbles are growing rapidly during its climbing. Nevertheless a satisfactory agreement was found between numerics and experiments.

Keywords: Two-Phase Flow · CFD · Volume of Fluid · Bubbles · OpenFoam.

1 Introduction

The two-phase flow problem emerges in many technical applications starting from production processes up to the energetics. The objective of this two-phase flow examination was motivated by the effort to understand and further control the bubble formation in the metal foaming processes. There are generally many technological production methods to obtain the cellular type structures e.g. the continuous gas injection in the melted materials containing mostly other stabilization components. Details about aspects of the cellular material production can be found e.g. in [1]. This paper is concerned with the study of rising gas bubble in stagnant liquid in the pursue of creating metal foam, where common

* This work was supported by the Ministry of Education, Youth and Sports of the Czech Republic and the European Union - European Structural and Investment Funds in the frames of Operational Programme Research Development and Education - project Hybrid Materials for Hierarchical Structures (HyHi, Reg. No. CZ.02.1.01/0.0/16-019/0000843).

ICCS Camera Ready Version 2019
To cite this paper please use the final published version:
DOI: 10.1007/978-3-030-22747-0_43

parameters such as gas bubble diameters, velocity and dimensionless parameters and Morton number were examined. Other non-dimensional relevant parameters used in the problem of the bubble dynamics investigation can be found in [6]. To validate the numerical results, two different experimental examination patterns defined by the Morton numbers 1.6 x 10^{-11} and 5.7 x 10^{-9} were tested. It was found experimentally, that for the higher Morton number it was possible to trap the gas bubbles under the surface of the liquid, while for the latter it was not possible to trap any gas bubbles under the surface of the liquid fluid. The numerical approach based on the a multi-phase flow model which was built on the conservation laws of mass, momentum and energy as well as the gas-phase volume fraction advection equation was successfully adopted for the bubble formation problems [2]. In the study of bubbles in [3] involving the dynamics of a bubble, it was found that the deformation predicted using the numerical calculation was a good fit for the experimental results. It also confirmed the dependence of the bubble aspect ratio on Weber and Morton numbers for the cases of spherical and ellipse bubbles. CFD approach was successfully used for prediction of the bubble formation in the bubbly liquid metal flows. The chosen numerical method is an immersed boundary method extended to deformable bubbles. Experimental and numerical results were found to be in very good agreement both for the disperse gas phase and for the continuous liquid metal phase [5]. Other techniques used for the multicomponent two-phase fluid mixtures in a closed system at constant temperature can be found in [4].

2 Problem formulation

Computational domain The computational domain is represented by the box L x B x H and it is illustrated in Fig. 1. The mesh is composed by hexahedral cells with spacing of 90 x 90 x 350 and with the total number of 2.835 mil. cells. The periodic boundary conditions are applied on all sides. The inlet/outlet boundary type condition is prescribed for the top of a box having zero values for all phases except the gas phase for which the input/output velocity magnitudes are calculated. For the bottom of the gas phase, the parabolic inlet velocity profile with the U_{max} is prescribed. The mesh is generated by the SnappyHexMesh. Because the hexahedral cells are only applied for the mesh generation, the non-orthogonality stays to be zero, the max. skewness is very small 3.52 x 10^{-13} and max. aspect ratio is 2.34. The mesh quality is suitable in respect to the pimple solver requirements.

Mathematical model and numerical approaches The mathematical model used in the calculation is based on volume of fluid approach (VOF). Generally, the material properties of the homogeneous mixture is prescribed by the volume fraction function for the phase 1, which is defined as

$$\alpha_1 = \frac{\Omega_1}{\Omega_1 + \Omega_2} \tag{1}$$

ICCS Camera Ready Version 2019
To cite this paper please use the final published version:
DOI: 10.1007/978-3-030-22747-0_43

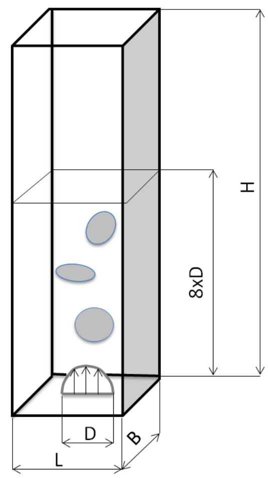

Fig. 1. Sketch of the computational domain with the size description.

where Ω_1 and Ω_2 are a volume of the phase 1 or 2, respectively. Analogously, the parameter for the phase 2 can be determined similarly or as simply $\alpha_2 = 1 - \alpha_1$. A conservation law of mass for each component separately must be also included. Furthermore, gravitational effects should be considered and included for liquid-phase wave problems as well. Finally, the underlying conservative part of the flow model can be expressed in the from 2.

$$\frac{\partial U}{\partial t} + \frac{\partial F_1}{\partial x} + \frac{\partial F_2}{\partial x} + \frac{\partial F_3}{\partial x} = G \tag{2}$$

where U is the vector of conservative variables, F is the flux function, and G are the source terms.

The calculation was carried out in OpenFOAM code using PIMPLE scheme. The Gauss linear scheme was applied for the most of all variables. The compressible Multiphase solver was used with varied time step determined by the stability condition based on the maximal Courant number of 0.25. The gas phase was treated as a ideal gas and the liquid phase as a perfect fluid.

Validation by experiments To validate numerical results, the experiments were carried out. The experiment test rig contains a glass water tank of dimensions 30 x 20 x 20 cm, that has a nozzle connected to a flow meter and an air compressor with controllable flow rate. A source of light is used to focus on the gas bubbles of which images are acquired by the means of the speed camera. A sheet of parchment paper is used as a light diffuser to decrease the contrast of the images making it possible to see the gas/liquid boundary in the bubble, using image processing software. It was possible to measure diameter of the bubble, velocity and several dimensionless parameters for several image frames,

ICCS Camera Ready Version 2019
To cite this paper please use the final published version:
DOI: 10.1007/978-3-030-22747-0_43

which later was imported into spreadsheet software to calculate changes through distance or time.

3 Results

Figure 2 shows numerically identified air bubble in the water formed at the nozzle located at the bottom and these bubbles were rising up due to force affects. The asymmetrical path of the bubbles is evident despite of the fact that the conditions are numerically symmetric. Similar feature of the bubble path is possible to observe experimentally. The deformation of the bubble shapes due to force acting is similar for experiment and CFD. Different calculated bubble shapes is possible to see on Fig. 2 (left) which correspond to shapes in experiment. However, the exactly match regarding bubble shapes in time and space is not possible to see it because of different time of the bubble formation.

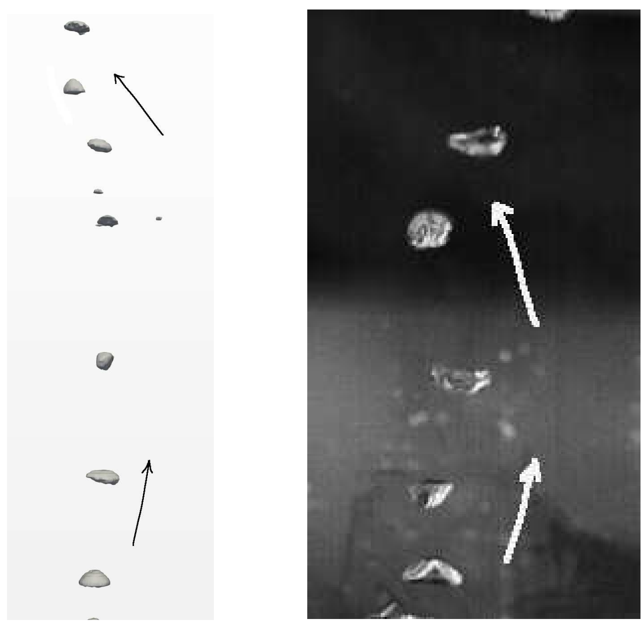

Fig. 2. Path of the bubbles for the air flow rate of 5 l/h examined numerically (left) and experimentally (right).

Figure 3 depicts the time series of bubble visualization in the liquid flow to help to identify the bubble dynamics. The air flow rate is about 5l/h and the time step is 0.3s. The bubble shapes change by time, it rotates and inclines. The flow of the liquid is illustrated by the vectors. At the particular position of the bubble, it is possible to observe the strong flow circulation of the liquid around

ICCS Camera Ready Version 2019
To cite this paper please use the final published version:
DOI: 10.1007/978-3-030-22747-0_43

the bubble. This circulating flow appears due to force imbalance acting on the bubble. The mesh used for calculations provides at least 10 points over the bubble diameter to resolve the shape of the bubbles sufficiently (this conclusion is based on the previous test calculations). The similar forms of the bubble identified by numerics were found by experiments as well.

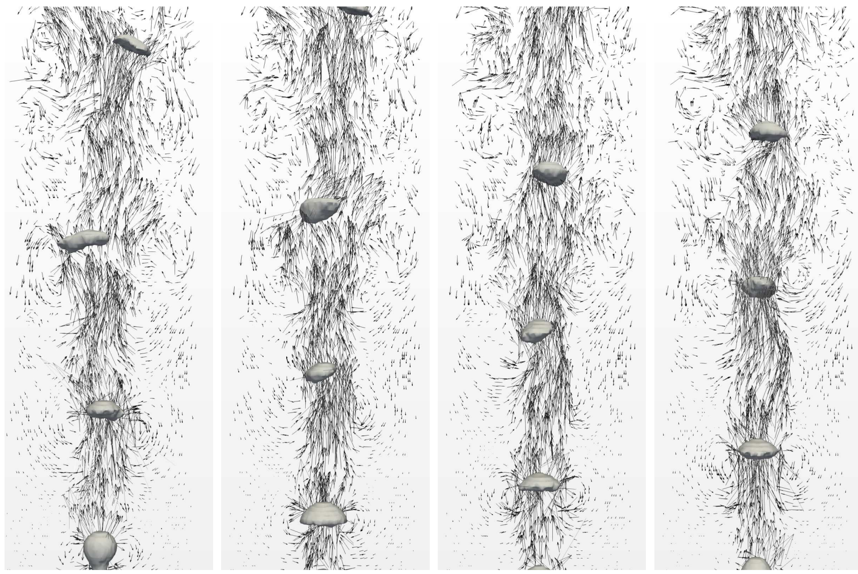

Fig. 3. Unsteady bubble dynamics for the air flow rate of 5l/h captured by the time step of 0.3s.

Figure 4 illustrates the change of the bubble diameter in time for the gas flow rate 5l/h. The diameter is scaled by the diameter of the nozzle. The time is scaled by the total time needed a bubble to reach surface of the liquid level. Time required by one bubble to reach the surface of the liquid in the tank is about 0.377 second, while the diameter of the nozzle is about 3mm. The numerical calculation overestimated the intensity of the bubble growth from the onset of the bubble up to the non-dimensional time 0.2. After that the bubble size oscillated about the non-dimensional diameter of 3. A growth of the bubble observed experimentally is significantly slower. The unique evaluation of the bubble diameters and Reynolds numbers were possible only for the cases in which the single bubbles are formed and travelled separately without interactions.

Figure 5 shows two different bubble shapes formed in the case in which the air flow rate reaches 130 l/h. In this case, no single travelling bubble is formed, but the big bubble is created at the bottom which quickly moves upwards. It interacts with the previous bubbles to be formed into the big structure. To observe the dynamics of the bubble is difficult because of the complexity of the flow. At

ICCS Camera Ready Version 2019
To cite this paper please use the final published version:
DOI: 10.1007/978-3-030-22747-0_43

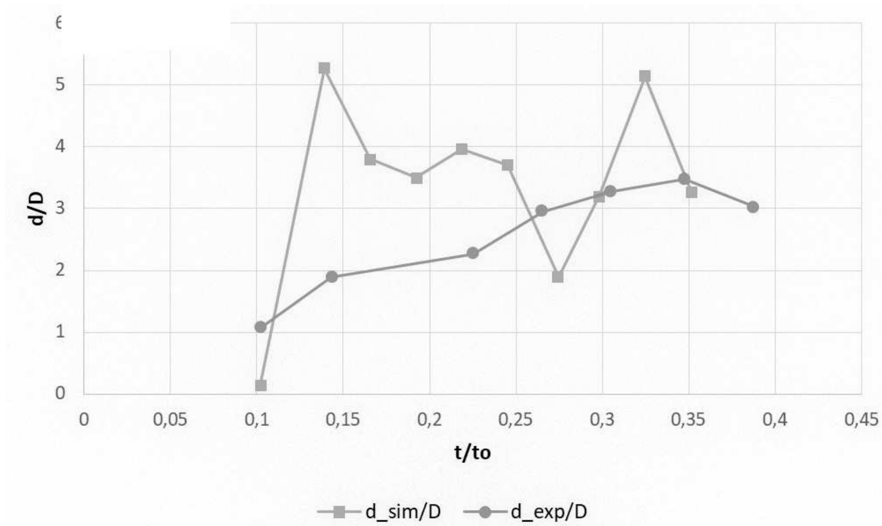

Fig. 4. Diameter of the formed bubbles in time.

the onset of the bubble different bubble shapes are formed before detachment from the input nozzle. The numerical simulation predicted bubble shapes well, however, without typical unsymmetrical feature observed experimentally. After the onset of the bubble and its detaching, the bubble starts to grow. This feature was observed experimentally and numerically, however, numerical results embodied slow growing process. This observed feature was not still further studied in details.

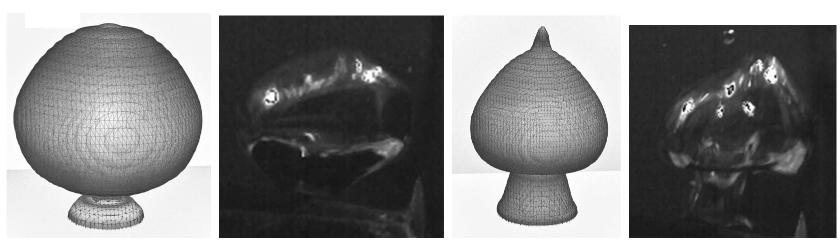

Fig. 5. Unsteady bubble dynamics for the air flow rate of 130l/h for different time examined numerically and experimentally (figures by the black background).

The diameter of the bubbles and terminal velocity were compared between experiments and numerics for the gas flow rate 130l/h. The experiment identified the averaged terminal velocity of about 0.4m/s, the numerics about 0.45 m/s.

ICCS Camera Ready Version 2019
To cite this paper please use the final published version:
DOI: 10.1007/978-3-030-22747-0_43

4 Conclusion

The gas-liquid flow problem defined by the low 5l/h and high 130l/h gas flow rates was studied numerically. The feasibility of the numerical approach based on the formulation of mass, moment and energy conservation with the volume of fluid model was clearly demonstrated by a satisfactory agreement between numerical and experimental results. The calculation was carried out in the code OpenFoam for the multi-phase compressible flow. A good agreement between experimental and numerical results was found for the gas flow rates of 5l/h and 130l/h. However, the comparison of the results was difficult because of the complex flow structures formed under conditions of the higher gas flow rates. From perspectives, the numerical simulation can be further applied for the different liquid phase with modified material properties (addition of the suitable chemical components) in order to find the impact of this material property change on the bubble formation and dynamics.

References

1. Rajak, D. K., Kumaraswamidhas, L.A., Das, S.: Technical Overview of Aluminum Alloy Foam. Material Science 48, 68–86 (2007).
2. Ma, Z.H., Causon, D.M., Qian, L., Mingham, C.G., Gu, H.B., Martnez Ferrer, P.: A compressible Multiphase Flow Model for Violent Aerated Wave Impact Problems. Proc. R. Soc. A vol. 470, (2017). https://doi.org/10.1098/20140542
3. Gumulya, M., Joshi., J.B., Utikar, R.P., Evans G.M., Pareek V.: Bubbles in viscous liquids: Time Dependent Dehaviour and Wake Characteristics. Chemical EngineeringScience 144, 298309 (2016).
4. Fan X., Kou J., Qiao Z., and Sun S., A Componentwise Convex Splitting Scheme for Diffuse Interface Models with Van der Waals and Peng–Robinson Equations of State. SIAM J. Sci. Comput. 39(1). http://doi.org/10.1137/16M1061552.
5. Krull, B., Strumpf, E., Keplinger, O., Shevchenko, N., Fröhlich, J., Eckert, S., Gerbeth, G.: Combined Experimental and Numerical Analysis of a Bubbly Liquid Metal Flow. Materials Science and Engineering 228 (2017). doi:10.1088/1757-899X/228/1/012006.
6. Jamialahmadi,M.,Branch,C., Muller-Steinhagen, H.: Terminal Bubble Rise Velocity in Liquids. Chemical Engineering Research and Design 72, 119–122 (1994).

ICCS Camera Ready Version 2019
To cite this paper please use the final published version:
DOI: 10.1007/978-3-030-22747-0_43